

## A New 6D Two-wing Hyperchaotic System: Dynamical Analysis, Circuit Design, and Synchronization

Michael Kopp <sup>\*,1</sup> and Inna Samuilik <sup>α,β,2</sup>

\*Institute for Single Crystals, NAS Ukraine, Nauky Ave. 60, Kharkiv 61072, Ukraine, <sup>α</sup>Institute of Life Sciences and Technologies, Daugavpils University, 13 Vienibas Street, LV-5401 Daugavpils, Latvia, <sup>β</sup>Institute of Applied Mathematics, Riga Technical University, LV-1048 Riga, Latvia.

**ABSTRACT** This paper introduces a novel 6D dynamic system derived from modified 3D Lorenz equations of the second type using state feedback control. While the original 3D equations are formally simpler than the classical Lorenz equations, they produce topologically more complex attractors with a two-winged butterfly structure. The proposed system contains the fewest terms compared to existing literature. These terms comprise two cross-product nonlinearities, two piecewise linear functions, six linear terms, and one constant. The new 6D hyperchaotic system exhibits a rich array of dynamic characteristics, including hidden attractors and dissipative behavior. A thorough dynamic analysis of this system was performed. In particular, bifurcation diagrams were constructed, Lyapunov exponents and dimensions were calculated, and multistability and offset boosting control were analyzed to understand the systems behavior further. An electronic circuit of the 6D hyperchaotic two-winged butterfly system was developed in the Multisim computer environment. The designed electronic circuit showed excellent agreement with the simulation results of the new 6D dynamic system. Synchronization of two identical 6D hyperchaotic systems was achieved using the active control method.

### KEYWORDS

Two-wing attractors  
Chaotic behavior  
Multistability  
Offset boosting control  
Circuit implementation  
Active control synchronization

### INTRODUCTION

Since Lorenz's discovery of a three-dimensional (3D) chaotic system (Lorenz 1963), chaos researchers have increasingly focused on studying dynamic systems with dimensions higher than three. This trend is driven by several reasons. Firstly, many physical phenomena cannot be adequately modeled by three-dimensional systems. Higher-dimensional systems can capture the more complex behaviors and interactions observed in fields such as hydrodynamic turbulence theory (Bohr *et al.* 1998), climate modeling (Soldatenko *et al.* 2021), and neurodynamics (Yin *et al.* 2022). Another reason is that higher-dimensional complex systems are often employed in cryptographic applications due to their increased unpredictability and difficulty in being reverse-engineered. This makes them ideal for secure communications and information encryption (Ramakrishnan 2018).

Numerous 4D hyperchaotic systems have been thoroughly documented in the literature. These include Lorenz's hyperchaotic

system (Jia 2007), Chen's hyperchaotic system (Chen *et al.* 2006), Liu's hyperchaotic system (Li 2009), the hyperchaotic Wang system (Wang and Chen 2008), the hyperchaotic Newton-Leipnik system (Ghosh and Bhattacharya 2010), and the hyperchaotic Vaidyanathan system (Vaidyanathan 2013). When constructing new hyperchaotic models, it is essential to consider several factors: the presence of multiple positive Lyapunov exponents, maintaining the smallest number of terms to meet the simplicity criteria established by researcher Sprott, and achieving the highest Kaplan-Yorke dimension.

Moreover, noteworthy among the issues in chaos theory are those of chaos control and synchronization. Chaos control for practical systems has been the subject of extensive research. The master, or drive system, and the slave, or response system, are two systems whose synchronization is the subject of the chaos synchronization problem. Control laws are created to address this issue by ensuring that, asymptotically over time, the output of the slave system tracks the output of the master system. Numerous techniques have been proposed, including active control (Jung *et al.* 2019; Bhat and Shikha 2019), adaptive control (Zhang *et al.* 2020; Tohidi *et al.* 2020; Vaidyanathan *et al.* 2014; Vaidyanathan and Volos 2015), backstepping control (Chu and Hu 2016), sliding mode control (Rajagopal *et al.* 2017a,b; Yousefpour *et al.* 2020), and

Manuscript received: 9 July 2024,

Revised: 31 October 2024,

Accepted: 9 November 2024.

<sup>1</sup>michaelkopp0165@gmail.com

<sup>2</sup>inna.samuilika@rtu.lv (Corresponding author).

■ **Table 1** List of recently cited 6D dynamical systems.

Reference	Total terms	Number nonlinear terms	Nature system
Benkouider <i>et al.</i> (2020)	17	2	Dissipative
Sabaghian <i>et al.</i> (2020)	15	2	Dissipative
Yang <i>et al.</i> (2020)	14	3	Dissipative
Al-Azzawi and Al-Obeidi (2021)	17	2	Dissipative
Aziz and Al-Azzawi (2022)	13	3	Dissipative
Al-Talib and Al-Azzawi (2022)	12	4	Dissipative
Al-Obeidi and Al-Azzawi (2022)	17	3	Dissipative
Michael Kopp and Andrii Kopp (2022)	17	2	Dissipative
Al-Talib and Al-Azzawi (2023a)	12	4	Dissipative
Al-Azzawi and Al-Obeidi (2023)	17	3	Dissipative
Kopp <i>et al.</i> (2023)	21	4	Dissipative
Khattar <i>et al.</i> (2024)	12	4	Dissipative
<b>This work</b>	<b>11</b>	<b>2</b>	<b>Dissipative</b>

so on. Recently, a passive control method has also been presented in the literature. In paper (Adiyaman *et al.* 2020), a passive control method was presented to stabilize a new 4D hyperchaotic system at zero equilibrium and synchronize two identical new 4D hyperchaotic systems with different initial conditions. In another paper (Emiroglu *et al.* 2022), a passive control method was described to stabilize and suppress chaos in a chaotic system. These control techniques can also be used to achieve different types of real chaos synchronization.

Recently, there has been a trend towards constructing hyperchaotic models with higher dimensions, such as 5D models with three positive Lyapunov exponents (Hu 2009; Yang and Chen 2013; Al-Azzawi and Hasan 2023), 6D models with four positive Lyapunov exponents (Al-Talib and Al-Azzawi 2023b), and 7D models with five positive Lyapunov exponents (Yang *et al.* 2018). Compared to standard 3D and 4D models, these higher-dimensional chaotic models exhibit greater unpredictability and complexity. As can be seen from Table 1, most 6D dynamical systems (Benkouider *et al.* 2020; Yang *et al.* 2020; Al-Azzawi and Al-Obeidi 2021; Al-Obeidi and Al-Azzawi 2022; Kopp *et al.* 2023) consist of 12 or more terms with dissipative nature, and no simple dissipative 6D hyperchaotic system consisting of only 11 terms has been found. In addition, the proposed 6D system has a simple structure, containing only two control parameters. This motivated us to search for a new hyperchaotic system that contains the smallest number of terms.

This manuscript consists of the following sections. The Introduction provides a brief overview of the current state of the problem. Section 2 gives the derivation of the new 6D hyperchaotic dynamic system using state feedback control. In Section 3, we examine the dynamic characteristics of the new 6D nonlinear system

by analyzing the fixed points, constructing bifurcation diagrams, and determining the spectrum and Lyapunov dimension. This section also delves into multistability and offset boosting control for the new system. Section 4 is dedicated to developing an electronic circuit for a hyperchaotic chaos generator using the Multisim environment. The circuit's operation was tested, and the simulation results were compared with those obtained in the Mathematica environment. Finally, in Section 5, we extend our focus to the numerical analysis of synchronization between two identical 6D hyperchaotic systems. We utilized the active control method (see, for example, Jung *et al.* 2019; Bhat and Shikha 2019) to achieve synchronization. The Conclusions section presents the main results obtained in this article.

## DERIVATION OF A NEW 6D HYPERCHAOTIC DYNAMIC SYSTEM

In this section, we outline a method to derive a new six-dimensional (6D) dynamical system from a modified Lorenz system (Elwakil *et al.* 2002) of the following form:

$$\begin{cases} \frac{dx_1}{dt} = a(-x_1 + x_2) \\ \frac{dx_2}{dt} = -x_3 \operatorname{sgn}(x_1) \\ \frac{dx_3}{dt} = |x_1| - 1 \end{cases} \quad (1)$$

Here  $|x|$  is the absolute value function, signum function  $\operatorname{sgn}(x)$  of

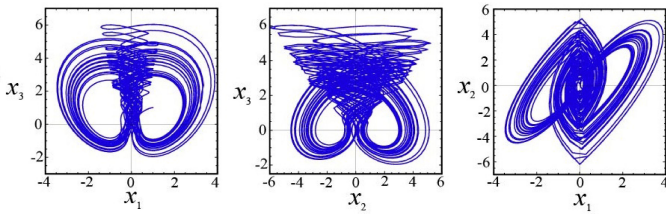


**Figure 1** Plots depict two-wing butterfly attractors of system (1) in phase planes  $x_1x_3$ ,  $x_2x_3$ , and  $x_1x_2$ , respectively.

a real number  $x$  is a piecewise function which is defined as follows:

$$\text{sgn}(x) = \begin{cases} -1 & \text{if } x < 0 \\ 0 & \text{if } x = 0 \\ 1 & \text{if } x > 0 \end{cases} \quad (2)$$

Figure 1 shows typical two-wing butterfly attractors in different phase planes for system (1) with  $a = 0.6$  and initial conditions  $x_1(0) = x_2(0) = x_3(0) = 1$ . The corresponding Lyapunov exponents are:

$$LE_1 = 0.191212, LE_2 \approx 0, LE_3 = -0.799337, \quad (3)$$

and the corresponding Kaplan-Yorke (or Lyapunov) dimension  $D_{KY} = 2.239$ . By incorporating a state variable  $x_4$  into the first equation of system (1) with a feedback strategy, we derive a four-dimensional (4D) dynamic system:

$$\begin{cases} \frac{dx_1}{dt} = a(-x_1 + x_2) + x_4 \\ \frac{dx_2}{dt} = -x_3 \text{sgn}(x_1) \\ \frac{dx_3}{dt} = |x_1| - 1 \\ \frac{dx_4}{dt} = -bx_1 \end{cases} \quad (4)$$

Here  $b$  is the new control parameter. Using a coupling strategy by adding state variables  $x_5$  and  $x_6$ , a six-dimensional (6D) hyperchaotic model is constructed, described as follows:

$$\begin{cases} \frac{dx_1}{dt} = a(-x_1 + x_2) + x_4 \\ \frac{dx_2}{dt} = -x_3 \text{sgn}(x_1) \\ \frac{dx_3}{dt} = -1 + |x_1| \\ \frac{dx_4}{dt} = -bx_1 \\ \frac{dx_5}{dt} = -x_5 + x_1x_4 \\ \frac{dx_6}{dt} = -x_6 + x_1x_3 \end{cases} \quad (5)$$

The resulting new 6D model of the dynamic system contains only 11 terms, which is one less than in recent paper (Al-Talib and Al-Azzawi 2023b). In addition to the linear terms, system (5) includes two nonlinearities ( $x_1x_4$ ,  $x_1x_3$ ) and two functions:  $\text{sgn}(x_1)$  and  $|x_1|$ . In this paper, we found that system (5) is hyperchaotic when the system parameters take the values  $a = 0.77$  and  $b = 0.45$ . For these parameter values and initial conditions (ICs)

$$x_1(0) = x_2(0) = x_3(0) = x_4(0) = x_5(0) = x_6(0) = 1, \quad (6)$$

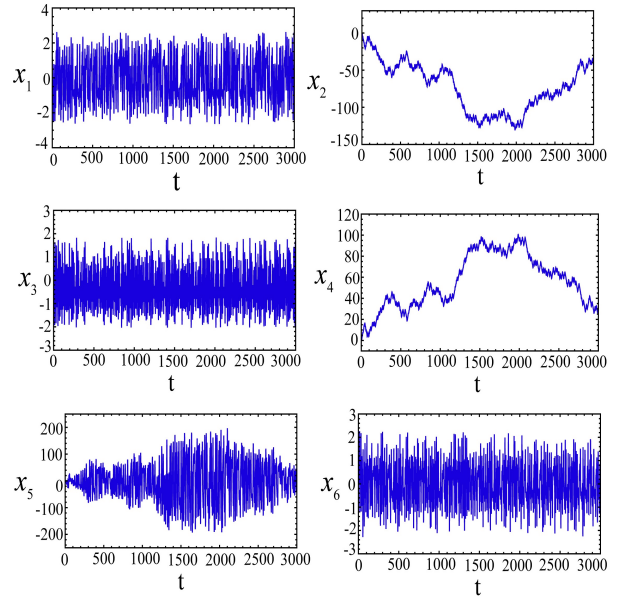


**Figure 2** Temporal diagrams for variables  $x_1, x_2, x_3, x_4, x_5, x_6$ .

all Lyapunov exponents of the new system (5) were calculated in the following form:

$$LE_1 = 0.13238, LE_2 = 0.01280, LE_3 = 0.00580 \approx 0, \\ LE_4 = -0.88594, LE_5 = -1.01495, LE_6 = -1.02017. \quad (7)$$

It is also of interest to obtain time series data for the new 6D dynamic system (5) with ICs (6). In the context of dynamic systems, time series data reflects the behavior or evolution of a system over time. Time series analysis can be used to study the state variables of the new model  $x_i$  ( $i = (1, 2, 3, 4, 5, 6)$ ) over time, as shown in Figure 2. Here, the random nature of the dependence of the variables  $x_i$  on time  $t$  is clearly visible.

Next, we start the dynamic analysis of the recently introduced systems (5).

## DYNAMICAL ANALYSIS

In this section, we explore some fundamental dynamic properties of the new proposed 6D system.

### Symmetry and dissipativity of the system

It is easy to verify that system (5) satisfies the following coordinate transformation  $T$ :

$$T: (x_1, x_2, x_3, x_4, x_5, x_6) \rightarrow (-x_1, -x_2, x_3, -x_4, x_5, -x_6).$$

This means that each trajectory is symmetrical about  $x_3$  and  $x_5$  axes, and the system (5) is invariant for a given transformation  $T$ .

The divergence of the vector field  $\Phi(\dot{x}_1, \dot{x}_2, \dot{x}_3, \dot{x}_4, \dot{x}_5, \dot{x}_6)$  of the system (5) can be calculated as:

$$\text{div} \Phi = \frac{\partial \dot{x}_1}{\partial x_1} + \frac{\partial \dot{x}_2}{\partial x_2} + \frac{\partial \dot{x}_3}{\partial x_3} + \frac{\partial \dot{x}_4}{\partial x_4} + \frac{\partial \dot{x}_5}{\partial x_5} + \frac{\partial \dot{x}_6}{\partial x_6} = -(a + 2) < 0, \\ \dot{x}_i \equiv \frac{dx_i}{dt}, \quad i = (1, 2, 3, 4, 5, 6). \quad (8)$$

■ Table 2 Lyapunov exponents for different values of the parameter  $a$ .

$a$	Lyapunov Exponents ( $LE_1, LE_2, LE_3, LE_4, LE_5, LE_6$ )	Signs	Behavior
0.005	<b>0.0340</b> , -0.0048, -0.0025, -0.0147, -1.00094, -1.0159	(0, -, -, -, -, -)	Periodic
0.15	<b>0.0199</b> , -0.0016, -0.0897, -0.0680, -1.0020, -1.0083	(0, -, -, -, -, -)	Periodic
0.3	0.0913, <b>0.0020</b> , <b>-0.0017</b> , -0.3713, -1.0116, -1.0086	(+, 0, 0, -, -, -)	Chaotic 2-torus
0.6	0.1484, 0.0111, <b>0.0076</b> , -0.7418, -1.0150, -1.0103	(+, +, 0, -, -, -)	Hyperchaotic
0.75	0.1367, <b>0.0014</b> , <b>-0.0005</b> , -0.8653, -1.0074, -1.0148	(+, 0, 0, -, -, -)	Chaotic 2-torus
0.77	0.1323, 0.0127, <b>0.0058</b> , -0.8859, -1.0149, -1.0201	(+, +, 0, -, -, -)	Hyperchaotic
1.5	<b>0.0085</b> , -0.0155, -0.0235, -0.9894, -1.0088, -1.4712	(0, -, -, -, -, -)	Periodic

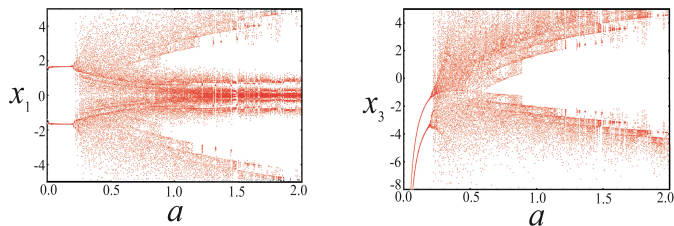


Figure 3 Bifurcation diagrams for  $x_1, x_3$  components of the system (5).

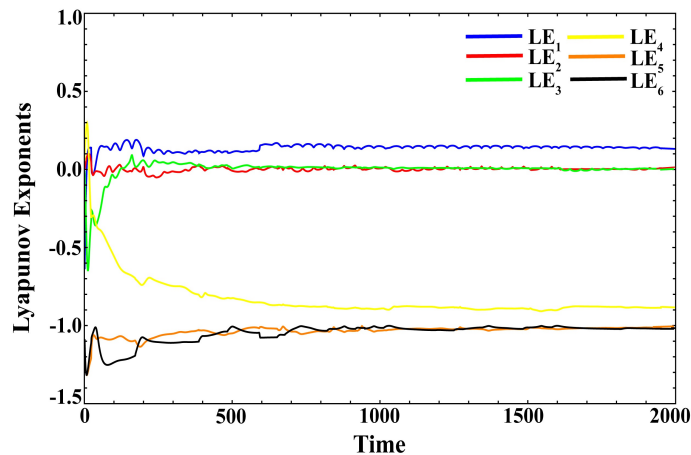


Figure 4 Lyapunov exponents for system (5).

According to Liouville's theorem, the phase volume  $V$  changes over time as follows:

$$\frac{dV}{dt} = \int \dots \int \operatorname{div} \Phi dx_1 dx_2 dx_3 dx_4 dx_5 dx_6 = -(a+2)V(t). \quad (9)$$

In this case, the phase volume exponentially diminishes to zero as time  $t$  approaches infinity:  $V(t) = V(0) \exp(-(a+2)t)$ . As a result, system (5) is dissipative, allowing for the emergence of attracting sets, or attractors.

#### Equilibrium points

The equilibrium states of a dynamic system (5) are found from the left-hand sides of the equations by setting  $\dot{x}_1 = \dot{x}_2 = \dot{x}_3 = \dot{x}_4 = \dot{x}_5 = \dot{x}_6 = 0$ :

$$\begin{cases} 0 = a(-\tilde{x}_1 + \tilde{x}_2) + \tilde{x}_4 \\ 0 = -\tilde{x}_3 \operatorname{sgn}(\tilde{x}_1) \\ 0 = -1 + |\tilde{x}_1| \\ 0 = -b\tilde{x}_1 \\ 0 = -\tilde{x}_5 + \tilde{x}_1\tilde{x}_4 \\ 0 = -\tilde{x}_6 + \tilde{x}_1\tilde{x}_3 \end{cases} \quad (10)$$

Solving the equations (10) under the assumption that  $a$  and  $b$  are non-zero parameters results in  $x_1 = 0$  from the fourth equation. Substituting this value into the third equation produces a contradiction  $-1 = 0$ , indicating the absence of equilibrium points in the system. Consequently, all attractors generated by system (5) are considered hidden attractors.

#### Bifurcation diagrams, analysis of Lyapunov exponents and dimension

Bifurcation diagrams represent changes in state variables of non-linear dynamic systems graphically. They provide insights into qualitative changes as control parameters are adjusted. We use Mathematica software to solve the equations outlined in (5) with the initial conditions from (6). In our analysis, we control the parameter  $a$  in the system (5), while keeping the parameter  $b$  fixed at  $b = 0.45$ . Figure 3 displays bifurcation diagrams for the  $x_1$  and  $x_3$  components of the system (5) as  $a$  varies within the interval  $a \in [0, 2]$ . These diagrams help identify stable regions and

regular behaviors (represented by individual points) within the system. They can also indicate areas where the system exhibits periodic or quasi-periodic behavior. Each branch in the diagram may correspond to different periodic orbits, reflecting various vibration modes. Additionally, bifurcation diagrams can illustrate period-doubling bifurcations as the parameter  $a$  changes. These bifurcations represent a sequence in which the system transitions from one periodic state to a period-doubling state, which can continue and may ultimately lead to chaotic behavior. As shown in the bifurcation diagram in Figure 3, there are two branches of regular oscillations: a lower (left) branch and an upper (right) branch. The left periodic attractor undergoes a period-doubling bifurcation, and a similar bifurcation occurs for the right attractor at the same value of  $a$ . In other words, the left and right attractors are mirror images of each other.

As is known, Lyapunov exponents (LEs) are an important criterion for describing the behavior and stability of dynamic systems. LEs characterize the rate of divergence or convergence of neighboring trajectories in a dynamic system. A dynamic system is assumed to be unstable or exhibit chaotic behavior when the LE is positive, and a negative exponent indicates a tendency toward stable equilibrium. Thus, by examining the sign of the LEs, one can classify the system's behavior as regular, quasi-regular (2-torus, 3-torus), chaotic, or hyperchaotic. The number of Lyapunov exponents corresponds to the dimensionality of the dynamical system. In the case of our system (5), there are six such indicators. Following the methodology (Binous and Zakia 2008), we computed LEs for specific values of parameter  $a$  at fixed parameter  $b = 0.45$  and ICs (6). Lyapunov exponents offer deep insights into how the system's dynamic behavior evolves with changes in the parameter  $a$ . According to Table 2, the dynamical behaviors of system (5) can be categorized into the following groups based on the Lyapunov exponents. In the future, we will be interested in the hyperchaotic behavior of the system (5) for the parameter value  $a = 0.77$ . In this case, the sum of all six Lyapunov exponents is  $L_1 + L_2 + L_3 + L_4 + L_5 + L_6 = -2.77 < 0$ . This suggests that system (5) exhibits dissipative behavior (see, for example, (Kozlovska et al. 2024)). It is easy to verify that a hyperchaotic system (5) at parameters  $a = 0.77, b = 0.45$  satisfies the condition (Singh and Roy 2016):

$$\sum_{i=1}^6 LE_i = \text{div} \Phi = -2.77. \quad (11)$$

Figure 4 illustrates the dynamics of the Lyapunov exponents ().

One of the most frequently used characteristics in the numerical modeling of dynamic systems is the Lyapunov dimension, proposed by Kaplan and Yorke (Frederickson et al. 1983). The Lyapunov dimension helps to identify the fractal dimension of a chaotic system, which is a measure of the complexity and entanglement of the system's attractor. Higher Lyapunov dimensions typically indicate more complex systems. For convenience, let us present the spectrum of the Lyapunov exponents in descending order:  $LE_1 > LE_2 > LE_3 > LE_4 > LE_5 > LE_6$  and calculate the Lyapunov Kaplan-Yorki dimension according to the following formula:

$$D_{KY} = \zeta + \frac{1}{|LE_{\zeta+1}|} \sum_{i=1}^{\zeta} LE_i = 3 + \frac{0.1509}{0.8859} \approx 3.17, \quad (12)$$

where  $\zeta$  is determined from the conditions

$$\sum_{i=1}^{\zeta} LE_i > 0 \Rightarrow \sum_{i=1}^3 LE_i = 0.1509, \quad \sum_{i=1}^{\zeta+1} LE_i = -0.735 < 0.$$

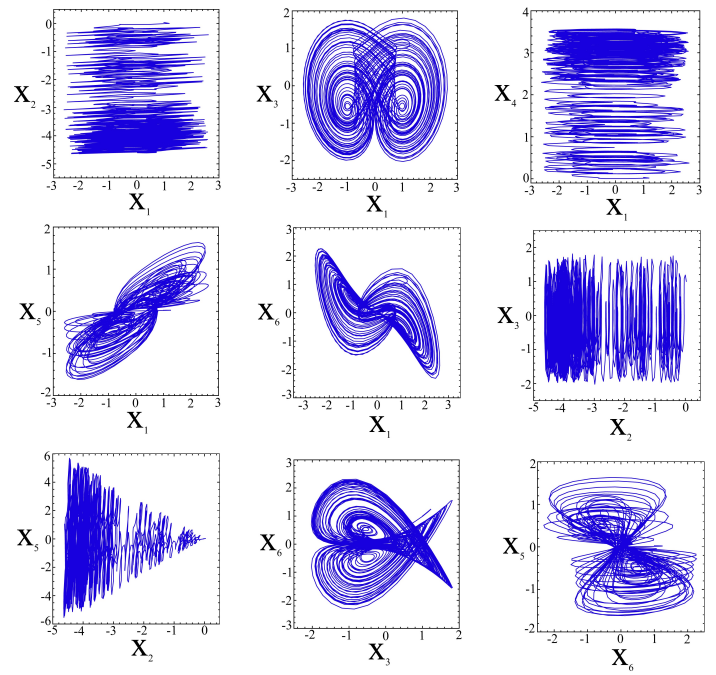


Figure 5 Hidden attractors of the new 6D rescaled system (13) in different planes.

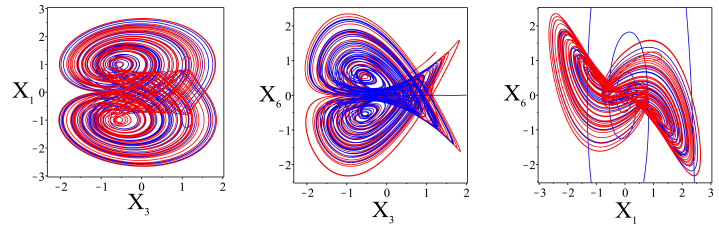


Figure 6 Plots demonstrating the multistability of two attractors in different phase planes with two different ICs given in Table 3.

Here  $\zeta$  is the number of first non-negative exponents Lyapunov in the spectrum. From (12), it is evident that the Lyapunov dimension is fractal, indicating that the trajectories of system (5) exhibit complex behavior.

### Visualizing phase portraits in the rescaled 6D dynamic system

As mentioned in the previous subsection, the dynamic system (5) can display hyperchaotic behavior. This makes the visual analysis of phase portraits for hyperchaotic attractors especially insightful. It is easy to see from Figure 2 that the temporal diagrams for the variables  $x_1, x_2, x_3, x_4, x_5$ , and  $x_6$  exhibit an aperiodic structure, a defining feature of chaotic systems. Implementing the hyperchaotic system (5) in an electronic circuit presents challenges, as the dynamic variables  $x_2, x_4$ , and  $x_5$  exceed the operational amplifiers' power supply limits. To address this, we scale the variables in the system (5) by setting  $x_2 = 30X_2, x_4 = 30X_4$ , and  $x_5 = 40X_5$ , while keeping  $x_1 = X_1, x_3 = X_3$ , and  $x_6 = X_6$ . This transformation results in the modified form of the hyperchaotic system (5) and ICs (6) in the following form:

■ **Table 3 Multistability of the system (13) with fixed parameters  $a=0.77$ ,  $b=0.45$  and various ICs.**

Figure planes	Initial Conditions	Color	Sign of LEs
$X_3X_1$	$(1, \frac{1}{30}, 1, \frac{1}{30}, \frac{1}{40}, 1)$	red	$(+, +, 0, -, -, -)$ hyperchaotic
$X_3X_1$	$(-1, -\frac{1}{30}, 1, -\frac{1}{30}, -\frac{1}{40}, 1)$	blue	$(+, +, 0, -, -, -)$ hyperchaotic
$X_3X_6$	$(1, \frac{1}{30}, 1, \frac{1}{30}, \frac{1}{40}, 1)$	red	$(+, +, 0, -, -, -)$ hyperchaotic
$X_3X_6$	$(5.2, -\frac{1}{3}, 3.5, \frac{1}{30}, -\frac{1}{40}, 1)$	blue	$(+, +, 0, -, -, -)$ hyperchaotic
$X_1X_6$	$(1, \frac{1}{30}, 1, \frac{1}{30}, \frac{1}{40}, 1)$	red	$(+, +, 0, -, -, -)$ hyperchaotic
$X_1X_6$	$(-5.2, -\frac{1}{3}, 3.5, -\frac{1}{30}, \frac{1}{40}, 1)$	blue	$(+, +, 0, -, -, -)$ hyperchaotic

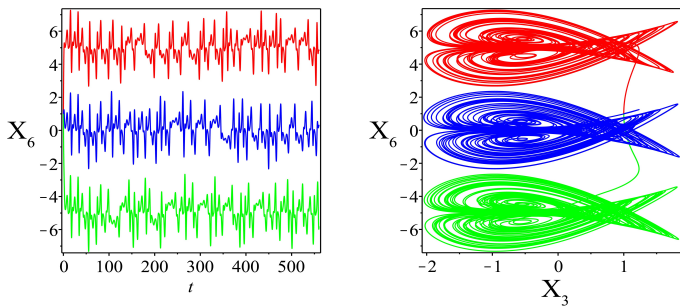


**Figure 7** Signal  $X_6$  and phase portrait in the plane  $X_3X_6$  for different values of the offset boosting controller  $k$ :  $k = 0$  (blue),  $k = 5$  (green),  $k = -5$  (red).

$$\begin{cases} \frac{dX_1}{dt} = a(-X_1 + 30X_2) + 30X_4 \\ \frac{dX_2}{dt} = -\frac{X_3}{30} \operatorname{sgn}(X_1) \\ \frac{dX_3}{dt} = -1 + |X_1| \\ \frac{dX_4}{dt} = -\frac{b}{30}X_1 \\ \frac{dX_5}{dt} = -X_5 + \frac{3}{4}X_1X_4 \\ \frac{dX_6}{dt} = -X_6 + X_1X_3 \end{cases} \quad (13)$$

$$\begin{aligned} X_1(0) = 1, X_2(0) = 1/30, X_3(0) = 1, X_4(0) = 1/30, \\ X_5(0) = 1/40, X_6(0) = 1. \end{aligned} \quad (14)$$

Systems (5) and (13) are equivalent, as the linear transformation adjusts the variables without affecting the intrinsic properties of the nonlinear system. Figure 5 illustrates the solutions of the transformed equations (13) given the initial conditions () and parameter values  $a = 0.77, b = 0.45$ . The phase portraits show hidden attractors in the different planes. Notably, the dynamic range of the variables  $x_2, x_4, x_5$  is considerably reduced compared to Figure 2. This reduction facilitates the practical implementation of electronic circuits using operational amplifiers, which operate within the typical voltage limits of  $-15V$  to  $+15V$ .

### Multistability and offset boosting control

Dynamic systems, as mathematical constructs used to describe complex phenomena across various scientific fields, can possess

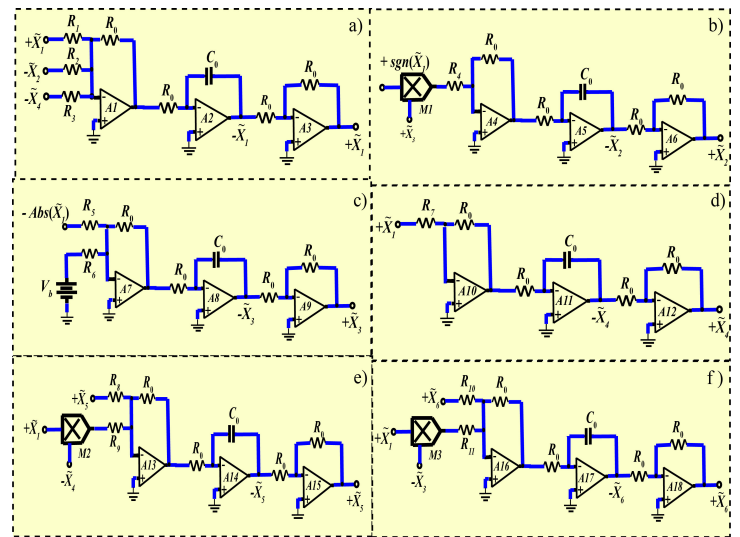


**Figure 8** Circuit modules implemented based on a system of equations (13): a)  $\tilde{X}_1$ , b)  $\tilde{X}_2$ , c)  $\tilde{X}_3$ , d)  $\tilde{X}_4$ , e)  $\tilde{X}_5$ , f)  $\tilde{X}_6$ .

multiple attractors. These attractors, which may be points, cycles, tori, or more complex chaotic structures, represent distinct states of the system. The specific attractor to which a system converges depends on its initial conditions, meaning small changes in these conditions can lead to different long-term behaviors. This leads to the concept of multistability, where several attractors coexist within the same set of system parameters.

In this subsection, we examine the multistability property of system (5), demonstrating how different attractors can coexist under the same system parameters when initial conditions are varied. Table 3 provides data for two attractors obtained by solving system (13) with identical control parameters  $a = 0.77, b = 0.45$  but different initial conditions. Figure 6 clearly illustrates the behavior of these two attractors based on the data from Table 3.

Offset boosting control has numerous applications in hyperchaotic systems. This method allows for flexible shifting of the attractor in a specific direction by introducing an offset, which holds significant engineering application value (Wen et al. 2021). Note that the state variable  $X_6$  appears only in the sixth equation of the proposed system, making it easy to control. Consequently, the  $X_6$  variable can be increased by introducing a  $k$  offset boosting controller, replacing  $X_6$  with  $X_6 + k$ . The sixth differential equation

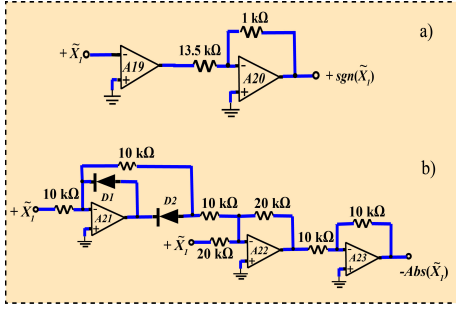


**Figure 9** Schematic diagrams for the implementation of functions: a) signum  $\text{sgn}(\cdot)$ ; b) absolute value  $|\cdot|$ .

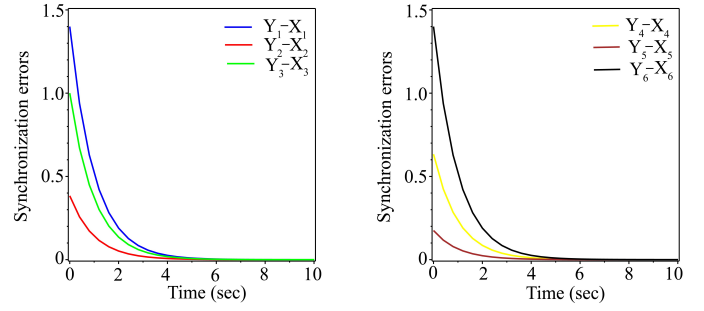


**Figure 11** Synchronization error behavior for 6D hyperchaotic drive and response systems.

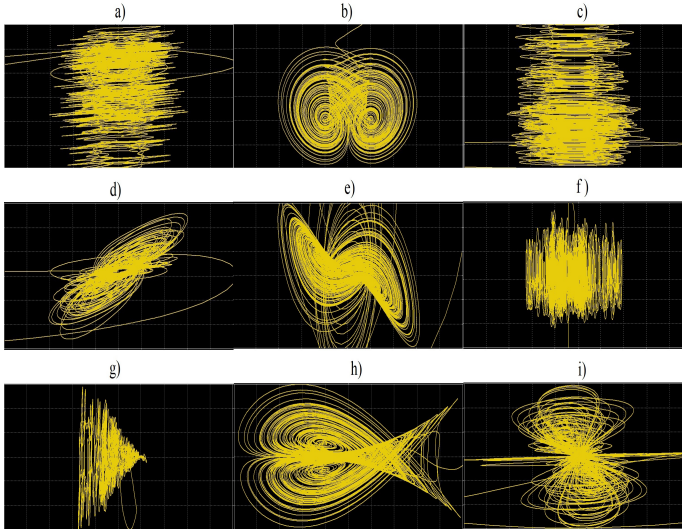


**Figure 10** Chaotic phase trajectories of an electronic circuit (Fig. 8) displayed in Multisim oscilloscopes: a)  $\tilde{X}_1\tilde{X}_2$ , b)  $\tilde{X}_1\tilde{X}_3$ , c)  $\tilde{X}_1\tilde{X}_4$ , d)  $\tilde{X}_1\tilde{X}_5$ , e)  $\tilde{X}_1\tilde{X}_6$ , f)  $\tilde{X}_2\tilde{X}_3$ , g)  $\tilde{X}_2\tilde{X}_5$ , h)  $\tilde{X}_3\tilde{X}_6$ , i)  $\tilde{X}_6\tilde{X}_5$ .

of system (13) can then be rewritten as follows:

$$\frac{dX_6}{dt} = -(X_6 + k) + X_1X_3. \quad (15)$$

Figure 7 depicts several positions of hyperchaotic attractors boosted with different  $k$  values in the  $X_3X_6$  plane. As shown on the left side of Figure 7, adjusting the bias gain control  $k$  converts the signal  $X_6$  from bipolar to unipolar. For a positive value of  $k$ , the attractors are shifted in the negative direction, while for a negative value of  $k$ , the attractors are shifted in the positive direction.

## CIRCUIT IMPLEMENTATION

For the practical implementation of the proposed new 6D hyperchaotic system (5) (or (13)), circuit modeling must be performed using Multisim software. According to Kirchhoff's law for electrical circuits, we can write the electrical analogue of the system (13)

as follows:

$$\begin{cases} C_1 \frac{dU_1}{d\tau} = -\frac{U_1}{R_{11}} + \frac{U_2}{R_{12}} + \frac{U_4}{R_{13}} \\ C_2 \frac{dU_2}{d\tau} = \frac{U_3 \text{sgn}(U_1)}{R_{21}K} \\ C_3 \frac{dU_3}{d\tau} = \frac{|U_1|}{R_{31}} - \frac{\tilde{V}_b}{R_{32}} \\ C_4 \frac{dU_4}{d\tau} = -\frac{U_1}{R_{41}} \\ C_5 \frac{dU_5}{d\tau} = \frac{U_1U_4}{R_{51}K} - \frac{U_5}{R_{52}} \\ C_6 \frac{dU_6}{d\tau} = \frac{U_1U_3}{R_{61}K} - \frac{U_6}{R_{62}} \end{cases} \quad (16)$$

where  $\tilde{V}_b$  is a stable DC voltage source to implement the constant ( $=1$ ) in a system (5),  $R_{ij}$  are resistors ( $i, j = 1, 2, 3, 4, 5, 6$ ),  $U_i(\tau)$  are voltage values,  $C_i$  are capacitors, and  $K$  is a scaling coefficient for the multiplier. We choose the normalized resistor as  $R_0 = 100\text{k}\Omega$  and the normalized capacitor as  $C_0 = 1\text{nF}$ . Then the time constant is equal to  $t_0 = R_0C_0 = 10^{-4}\text{s}$ . We rescale the state variables of the system (16) as follows  $U_1 = U_0\tilde{X}_1, U_2 = U_0\tilde{X}_2, U_3 = U_0\tilde{X}_3, U_4 = U_0\tilde{X}_4, U_5 = U_0\tilde{X}_5, U_6 = U_0\tilde{X}_6, K = U_0K'$ , and  $\tau = t_0t$ . Next, we can write equations (16) in a dimensionless form. By substituting  $R_0, C_1 = C_2 = C_3 = C_4 = C_5 = C_6 = C_0$ , and  $K' = 10$  into (16) and comparing numerical values before the output voltages of the system (13), we get the value of resistors:

$$\begin{cases} \frac{d\tilde{X}_1}{dt} = -\frac{100\text{k}}{R_1}\tilde{X}_1 + \frac{100\text{k}}{R_2}\tilde{X}_2 + \frac{100\text{k}}{R_3}\tilde{X}_4 \\ \frac{d\tilde{X}_2}{dt} = -\frac{100\text{k}}{R_4 \cdot 10}\tilde{X}_3 \text{sgn}(\tilde{X}_1) \\ \frac{d\tilde{X}_3}{dt} = \frac{100\text{k}}{R_5}|\tilde{X}_1| - \frac{100\text{k}}{R_6}V_b \\ \frac{d\tilde{X}_4}{dt} = -\frac{100\text{k}}{R_7}\tilde{X}_1 \\ \frac{d\tilde{X}_5}{dt} = \frac{100\text{k}}{R_9 \cdot 10}\tilde{X}_1\tilde{X}_4 - \frac{100\text{k}}{R_8}\tilde{X}_5 \\ \frac{d\tilde{X}_6}{dt} = \frac{100\text{k}}{R_{11} \cdot 10}\tilde{X}_1\tilde{X}_3 - \frac{100\text{k}}{R_{10}}\tilde{X}_6 \end{cases} \quad (17)$$

where

$$\begin{aligned} R_1 &= 129.87\text{k}\Omega, R_2 = 4.329\text{k}\Omega, R_3 = 3.333\text{k}\Omega, R_4 = 300\text{k}\Omega, \\ R_5 &= R_6 = 100\text{k}\Omega, R_7 = 6.666\text{M}\Omega, R_8 = 100\text{k}\Omega, \end{aligned}$$

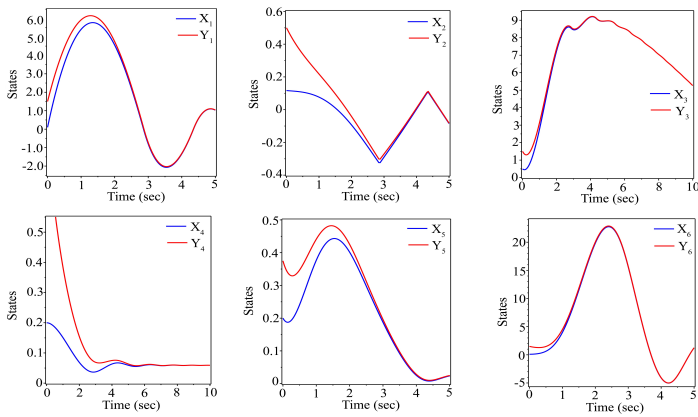


**Figure 12** Synchronization of the states for 6D hyperchaotic drive and response systems.

$$R_9 = 13.33k\Omega, R_{10} = 100k\Omega, R_{11} = 10k\Omega.$$

Figure 8 presents analog circuit modules for the equations of system (17), which consists of standard components such as resistors (R), capacitors (C), diodes D1, D2 (1N4001), multipliers M1-M3 (AD633), operational amplifiers A1-A23 (TL084ACN), and a supply voltage of  $\pm 15V$ . The constant 1 is implemented using a constant voltage source  $V_b = 1V$ . In the modules shown in Figures 8b and 8c, we used standard electronic circuits that simulate the signum  $\text{sgn}(\cdot)$  (see, for example, (Yu *et al.* 2008)) and absolute value  $|\cdot|$  functions (Sedra and Smith 1998), which are presented in Figure 9. Figure 10 presents the simulation results from Multisim of an electronic circuit, displaying hyperchaotic attractors of system (17) in various planes. These results align with those from the Mathematica simulation shown in Figure 5, confirming the feasibility of the proposed circuit.

### ACTIVE CONTROL SYNCHRONIZATION

Certainly, after developing a new chaotic oscillator based on 6D nonlinear dynamic equations, it is crucial to investigate the synchronization capabilities of this system to ensure its practical applicability. In this section, we examine the active control synchronization of two identical 6D hyperchaotic systems. System (13) was chosen as the drive system, while the response system is described as follows:

$$\begin{cases} \frac{dY_1}{dt} = a(-Y_1 + 30Y_2) + 30Y_4 + u_1 \\ \frac{dY_2}{dt} = -\frac{Y_3}{30}\text{sgn}(Y_1) + u_2 \\ \frac{dY_3}{dt} = -1 + |Y_1| + u_3 \\ \frac{dY_4}{dt} = -\frac{b}{30}Y_1 + u_4 \\ \frac{dY_5}{dt} = -Y_5 + \frac{3}{4}Y_1Y_4 + u_5 \\ \frac{dY_6}{dt} = -Y_6 + Y_1Y_3 + u_6 \end{cases} \quad (18)$$

where  $Y_1, Y_2, Y_3, Y_4, Y_5, Y_6$  are the states and  $u_1, u_2, u_3, u_4, u_5, u_6, u_7$  are active controllers that we will define later. Our objective is to synchronize the signals of both the drive and response systems, even when their initial conditions differ. The state errors are defined as  $e_i(t) = Y_i(t) - X_i(t)$ , for  $(i = 1, 2, 3, 4, 5, 6)$ . By subtracting

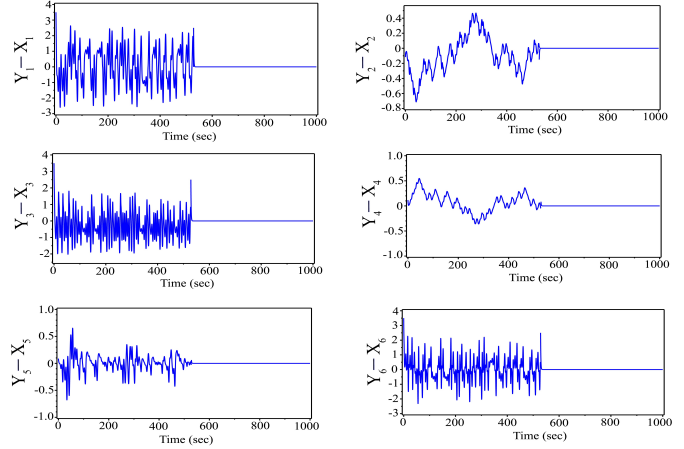


**Figure 13** Time evolution of the synchronization errors with controllers deactivated ( $t < 520s$ ) and activated ( $t > 520s$ ).

the drive system (13) from the response system (18), we obtain the error system as follows:

$$\begin{cases} \dot{e}_1 = a(-e_1 + 30e_2) + 30e_4 + u_1 \\ \dot{e}_2 = -\frac{1}{30}(Y_3\text{sgn}(Y_1) - X_3\text{sgn}(X_1)) + u_2 \\ \dot{e}_3 = |Y_1| - |X_1| + u_3 \\ \dot{e}_4 = -\frac{b}{30}e_1 + u_4 \\ \dot{e}_5 = \frac{3}{4}(Y_1Y_4 - X_1X_4) - e_5 + u_5 \\ \dot{e}_6 = (Y_1Y_3 - X_1X_3) - e_6 + u_6 \end{cases} \quad (19)$$

Next, we define active control functions aimed at producing an asymptotically stable error system, thereby achieving synchronization of the novel 6D hyperchaotic systems. The selected active control functions are detailed below:

$$\begin{cases} u_1 = -e_1 + ae_1 - 30ae_2 - 30e_4 \\ u_2 = -e_2 + \frac{1}{30}(Y_3\text{sgn}(Y_1) - X_3\text{sgn}(X_1)) \\ u_3 = -e_3 - (|Y_1| - |X_1|) \\ u_4 = -e_4 + \frac{b}{30}e_1 \\ u_5 = -\frac{3}{4}(Y_1Y_4 - X_1X_4) \\ u_6 = -(Y_1Y_3 - X_1X_3) \end{cases} \quad (20)$$

Then, the dynamic equations of the error system are as follows:

$$\begin{cases} \dot{e}_1 = -e_1 \\ \dot{e}_2 = -e_2 \\ \dot{e}_3 = -e_3 \\ \dot{e}_4 = -e_4 \\ \dot{e}_5 = -e_5 \\ \dot{e}_6 = -e_6 \end{cases} \quad (21)$$

Upon applying the proposed active control functions (20), the error system transforms into a linear form. For convenience, we express

this in matrix form as follows:

$$\begin{pmatrix} \dot{e}_1 \\ \dot{e}_2 \\ \dot{e}_3 \\ \dot{e}_4 \\ \dot{e}_5 \\ \dot{e}_6 \end{pmatrix} = \begin{pmatrix} -1 & 0 & 0 & 0 & 0 & 0 \\ 0 & -1 & 0 & 0 & 0 & 0 \\ 0 & 0 & -1 & 0 & 0 & 0 \\ 0 & 0 & 0 & -1 & 0 & 0 \\ 0 & 0 & 0 & 0 & -1 & 0 \\ 0 & 0 & 0 & 0 & 0 & -1 \end{pmatrix} \begin{pmatrix} e_1 \\ e_2 \\ e_3 \\ e_4 \\ e_5 \\ e_6 \end{pmatrix} \quad (22)$$

It can be easily verified that all eigenvalues of the state matrix (22) are negative. Therefore, according to the Routh-Hurwitz criterion, the error system is stable, ensuring synchronization between the drive system (13) and the response system (18).

### Numerical simulation

The nonlinear equations (13) and (18) were solved using the 4th-5th order Runge-Kutta-Fehlberg (rkf45) method in the Maple computing environment with the fixed parameters  $a = 0.77$ ,  $b = 0.45$ . The drive system (13) was initialized with the following conditions:

$$\begin{aligned} X_1(0) &= \frac{1}{10}, X_2(0) = \frac{7}{60}, X_3(0) = \frac{1}{2}, X_4(0) = \frac{1}{5}, \\ X_5(0) &= \frac{1}{5}, X_6(0) = \frac{1}{10}, \end{aligned} \quad (23)$$

and the response system was initialized with:

$$\begin{aligned} Y_1(0) &= \frac{3}{2}, Y_2(0) = \frac{1}{2}, Y_3(0) = \frac{3}{2}, Y_4(0) = \frac{5}{6}, \\ Y_5(0) &= \frac{3}{8}, Y_6(0) = \frac{3}{2}. \end{aligned} \quad (24)$$

Figure 11 illustrates the error curves resulting from the synchronization between the drive and response systems, showcasing the exponential convergence of synchronization errors  $e_i$  to zero over time. In Figure 12, the behavior of each state in both the drive and response systems is depicted, demonstrating the convergence of trajectories within a short time and indicating synchronization in these hyperchaotic systems.

For a clear representation of synchronization using the active control method, we select the following initial conditions for the drive system (13) and response system (18):

$$\begin{aligned} X_1(0) &= 1, X_2(0) = \frac{1}{30}, X_3(0) = 1, X_4(0) = \frac{1}{30}, \\ X_5(0) &= \frac{1}{40}, X_6(0) = 1, \\ Y_1(0) &= \frac{7}{2}, Y_2(0) = -\frac{7}{60}, Y_3(0) = \frac{7}{2}, Y_4(0) = \frac{7}{60}, \\ Y_5(0) &= \frac{7}{80}, Y_6(0) = \frac{7}{2}. \end{aligned} \quad (25)$$

Ensure that the active controllers are switched on at  $t = 520$  seconds. The results depicted in Figure 13 indicate that the error system states exhibit chaotic behavior over time when the active controllers are deactivated (at  $t < 520$  s), suggesting a lack of synchronization. At  $t \geq 520$  s, the controllers are activated, and we can see that the synchronization error states quickly converge to zero.

Thus, simulation findings demonstrate the ability of the active controllers (20) to synchronize two identical 6D hyperchaotic systems starting from various initial conditions.

## CONCLUSION

This work obtained a new 6D dynamic system with the smallest number of terms (only 11) compared to the existing 6D dynamic systems in the literature (see Tab. 1). It was found that the new dynamic system has no equilibrium points, which may lead to the formation of hidden attractors. For specific values of the system parameters, a hyperchaos regime was discovered, for which all Lyapunov exponents and the Kaplan-York dimension were calculated. The presence of two positive Lyapunov exponents indicates the complexity of the new 6D dynamic system. In addition, extensive studies of the dynamic properties of the system were carried out, including bifurcation diagrams, phase portraits, Lyapunov exponents, multistability, and offset boosting control. The electronic circuit of the proposed 6D system was designed using the Multisim 14 software. The results of the electronic circuit simulation are consistent with those obtained in the Mathematica environment. Finally, the synchronization between the two identical new 6D hyperchaotic systems was achieved by developing appropriate active controllers. The new system has promising applications in the field of encryption and decryption of information signals.

### Acknowledgments

We thank three anonymous reviewers for their valuable suggestions and comments.

### Availability of data and material

Not applicable.

### Conflicts of interest

The authors declare that there is no conflict of interest regarding the publication of this paper.

### Ethical standard

The authors have no relevant financial or non-financial interests to disclose.

## LITERATURE CITED

- Adıyaman, Y., S. Emiroğlu, M. K. Uçar, and M. Yıldız, 2020 Dynamical analysis, electronic circuit design and control application of a different chaotic system. *Chaos Theory and Applications* **2**: 10–16.
- Al-Azzawi, S. F. and A. S. Al-Obeidi, 2021 Chaos synchronization in a new 6d hyperchaotic system with self-excited attractors and seventeen terms. *Asian-European Journal of Mathematics* **14**: 2150085.
- Al-Azzawi, S. F. and A. S. Al-Obeidi, 2023 Dynamical analysis and anti-synchronization of a new 6d model with self-excited attractors. *Applied Mathematics-A Journal of Chinese Universities* **38**: 27–43.
- Al-Azzawi, S. F. and A. M. Hasan, 2023 New 5d hyperchaotic system derived from the spott c system: Properties and anti synchronization. *Journal of Intelligent Systems and Control* **2**: 110–122.
- Al-Obeidi, A. S. and S. F. Al-Azzawi, 2022 A novel six-dimensional hyperchaotic system with self-excited attractors and its chaos synchronisation. *International Journal of Computing Science and Mathematics* **15**: 72–84.
- Al-Talib, Z. S. and S. F. Al-Azzawi, 2022 A new simple 6d hyperchaotic system with nonhyperbolic equilibrium and its electronic circuit. In *2022 Int. Conf. Computer Sci. Software Engineering (CSASE)* pp. 369–374.

- Al-Talib, Z. S. and S. F. Al-Azzawi, 2023a A new simple 6d hyperchaotic system with hyperbolic equilibrium and its electronic circuit. *Iraqi Journal for Computer Science and Mathematics* **4**: 155–166.
- Al-Talib, Z. S. and S. F. Al-Azzawi, 2023b A new simple 6d hyperchaotic system with hyperbolic equilibrium and its electronic circuit. *Iraqi Journal For Computer Science and Mathematics* **4**: 155–166.
- Aziz, S. M. and S. F. Al-Azzawi, 2022 A novel simple 6d hyperchaotic system with hidden attractors. In 2022 Int. Conf. Computer Sci. Software Engineering (CSASE) pp. 7–12.
- Benkouider, K., T. Bouden, M. E. Yalcin, and S. Vaidyanathan, 2020 A new family of 5d, 6d, 7d and 8d hyperchaotic systems from the 4d hyperchaotic vaidyanathan system, the dynamic analysis of the 8d hyperchaotic system with six positive lyapunov exponents and an application to secure communication design. *International Journal of Modelling, Identification and Control* **35**: 241–257.
- Bhat, M. A. and M. Shikha, 2019 Complete synchronisation of non-identical fractional order hyperchaotic systems using active control. *International Journal of Automation and Control* **13**: 140–157.
- Binous, H. and N. Zakia, 2008 An improved method for lyapunov exponents computation. <https://library.wolfram.com/infocenter/MathSource/7109/>.
- Bohr, T., M. H. Jensen, G. Paladin, and A. Vulpiani, 1998 *Dynamical Systems Approach to Turbulence*. Cambridge Nonlinear Science Series, Cambridge University Press.
- Chen, A., J. Lu, J. Lu, and S. Yu, 2006 Generating hyperchaotic lu attractor via state feedback control. *Physica A* **364**: 103–110.
- Chu, J. and W. W. Hu, 2016 Control chaos for permanent magnet synchronous motor base on adaptive backstepping of error compensation. *International Journal of Automation and Computing* **9**: 163–174.
- Elwakil, A. S., S. Ozoguz, and M. P. Kennedy, 2002 Creation of a complex butterfly attractor using a novel lorenz-type system. *IEEE Transactions on Circuits and Systems I* **49**: 527–530.
- Emiroglu, S., A. Akgül, Y. Adı yaman, T. E. Gümüüş, Y. Uyaroglu, et al., 2022 A new hyperchaotic system from t chaotic system: dynamical analysis, circuit implementation, control and synchronization. *Circuit World* **48**: 265–277.
- Frederickson, P., J. L. Kaplan, E. D. Yorke, and J. A. Yorke, 1983 The liapunov dimension of strange attractors. *Journal of differential equations* **92**: 185–207.
- Ghosh, D. and S. Bhattacharya, 2010 Projective synchronization of new hyperchaotic system with fully unknown parameters. *Nonlinear Dynamics* **61**: 11–21.
- Hu, G., 2009 Generating hyperchaotic attractors with three positive lyapunov exponents via state feedback control. *International Journal of Bifurcation and Chaos* **19**: 651–660.
- Jia, Q., 2007 Hyperchaos generated from the lorenz chaotic system and its control. *Physics Letters A* **366**: 217–222.
- Jung, W., S. J. Elliot, and J. Cheer, 2019 Local active control of road noise inside a vehicle. *Mechanical Systems and Signal Processing* **121**: 144–157.
- Khattar, D., N. Agrawal, and M. Sirohi, 2024 Qualitative analysis of a new 6d hyper-chaotic system via bifurcation, the poincare notion, and its circuit implementation. *Indian Journal of Physics* **98**: 259–273.
- Kopp, M. I., A. V. Tur, and V. V. Yanovsky, 2023 Chaotic dynamics of magnetic fields generated by thermomagnetic instability in a nonuniformly rotating electrically conductive fluid. *Journal of Physical Studies* **27**: 2403.
- Kozlovska, O., F. Sadyrbaev, and I. I. Samuilik, 2024 A new 3d chaotic attractor in gene regulatory network. *Mathematics* **12**: 100.
- Li, X., 2009 Modified projective synchronization of a new hyperchaotic system via nonlinear control. *Communications in Theoretical Physics* **52**: 274–278.
- Lorenz, E. N., 1963 Deterministic nonperiodic flow. *Journal of atmospheric sciences* **20**: 130–141.
- Michael Kopp and Andrii Kopp, 2022 A new 6d chaotic generator: Computer modelling and circuit design. *International Journal of Engineering and Technology Innovation* **12**: 288–307.
- Rajagopal, K., L. Guessas, S. Vaidyanathan, A. Karthikeyan, and A. Srinivasan, 2017a Dynamical analysis and fpga implementation of a novel hyperchaotic system and its synchronization using adaptive sliding mode control and genetically optimized pid control. *Mathematical Problems in Engineering* **2017**: 1–14.
- Rajagopal, K., G. Laarem, A. Karthikeyan, and A. Srinivasan, 2017b Fpga implementation of adaptive sliding mode control and genetically optimized pid control for fractional-order induction motor system with uncertain load. *Advances in Difference Equations* **2017**: 1–20.
- Ramakrishnan, R., 2018 *Chaos and its applications to Communication Systems*. Scholars' Press, Cambridge.
- Sabaghian, A., S. Balochian, and M. Yaghoobi, 2020 Synchronisation of 6d hyper-chaotic system with unknown parameters in the presence of disturbance and parametric uncertainty with unknown bounds. *Connection Science* **32**: 362–383.
- Sedra, A. S. and K. C. Smith, 1998 *Microelectronics Circuits, 4th ed.* Oxford University Press, New York.
- Singh, J. P. and B. K. Roy, 2016 The nature of lyapunov exponents is (+, +, -, -), is it a hyperchaotic system? *Chaos, Solitons & Fractals* **92**: 73–85.
- Soldatenko, S., A. Bogomolov, and A. Ronzhin, 2021 Mathematical modelling of climate change and variability in the context of outdoor ergonomics. *Mathematics* **9**.
- Tohidi, S., Y. Yildiz, and I. Kolmanovsky, 2020 Adaptive state observers for incrementally quadratic nonlinear systems with application to chaos synchronization. *Automatica* **121**: 1–11.
- Vaidyanathan, S., 2013 A ten-term novel 4d hyperchaotic system with three quadratic nonlinearities and its control. *International Journal of Control Theory and Applications* **6**: 97–109.
- Vaidyanathan, S. and C. K. Volos, 2015 Analysis and adaptive control of a novel 3-d conservative no-equilibrium chaotic system. *Archives of Control Sciences* **25**: 333–353.
- Vaidyanathan, S., C. K. Volos, and V. T. Pham, 2014 Hyperchaos, adaptive control and synchronization of a novel 5-d hyperchaotic system with three positive lyapunov exponents and its spice implementation. *Archives of Control Sciences* **24**: 409–446.
- Wang, J. and Z. Chen, 2008 A novel hyperchaotic system and its complex dynamics. *International Journal of Bifurcation and Chaos* **18**: 3309–3324.
- Wen, J., Y. Feng, X. Tao, , and Y. Cao, 2021 Dynamical analysis of a new chaotic system: Hidden attractor, coexisting-attractors, offset boosting, and dsp realization. *IEEE Access* **9**: 167920–167927.
- Yang, L., Q. Yang, and G. Chen, 2020 Hidden attractors, singularly degenerate heteroclinic orbits, multistability and physical realization of a new 6d hyperchaotic system. *Communications in Nonlinear Science and Numerical Simulation* **90**: 105362.
- Yang, Q. and C. Chen, 2013 A 5d hyperchaotic system with three positive lyapunov exponents coined. *International Journal of*

- Bifurcation and Chaos **23**: 1350109.
- Yang, Q., D. Zhu, and L. Yang, 2018 A new 7d hyperchaotic system with five positive lyapunov exponents coined. International Journal of Bifurcation and Chaos **28**: 1850057.
- Yin, X., J. Chen, W. Yu, Y. Huang, W. Wei, *et al.*, 2022 Five-dimensional memristive hopfield neural network dynamics analysis and its application in secure communication. Circuit World **50**: 67–81.
- Yousefpour, A., A. H. Hosseinloo, M. R. H. Yazdi, and A. Bahrami, 2020 Disturbance observer-based terminal sliding mode control for effective performance of a nonlinear vibration energy harvester. Journal of Intelligent Material Systems and Structures **31**: 1495–1510.
- Yu, S., W. K. S. Tang, J. Lu, and G. Chen, 2008 Multi-wing butterfly attractors from the modified lorenz systems. 2008 IEEE International Symposium on Circuits and Systems (ISCAS), Seattle, WA, USA pp. 768–771.
- Zhang, H., W. Zhang, Y. Zhao, and M. Ji, 2020 Adaptive state observers for incrementally quadratic nonlinear systems with application to chaos synchronization. Circuits, Systems, and Signal Processing **39**: 1290–1306.

**How to cite this article:** Kopp, M. I., and Samuilik, I. A New 6D Two-wing Hyperchaotic System: Dynamical Analysis, Circuit Design, and Synchronization. *Chaos Theory and Applications*, 6(4), 273- 283, 2024.

**Licensing Policy:** The published articles in CHTA are licensed under a [Creative Commons Attribution-NonCommercial 4.0 International License](https://creativecommons.org/licenses/by-nc/4.0/).

